Journal of Medical Ultrasonics (2019) 46:367–375
https://doi.org/10.1007/s10396-019-00940-8

ORIGINAL ARTICLE—PHYSICS & ENGINEERING

Spectral analysis framework for compressed sensing ultrasound signals

Jaeyoon Shim[1] · Don Hur[1] · Hyungsuk Kim[1]

Received: 22 June 2018 / Accepted: 22 February 2019 / Published online: 6 April 2019

Abstract

Purpose Compressed sensing (CS) is the theory of the recovery of signals that are sampled below the Nyquist sampling rate. We propose a spectral analysis framework for CS data that does not require full reconstruction for extracting frequency characteristics of signals by an appropriate basis matrix.

Methods The coefficients of a basis matrix already contain the spectral information for CS data, and the proposed framework directly utilizes them without completely restoring original data. We apply three basis matrices, i.e., DCT, DFT, and DWT, for sampling and reconstructing processes, subsequently estimating the attenuation coefficients to validate the proposed method. The estimation accuracy and precision, as well as the execution time, are compared using the reference phantom method (RPM).

Results The experiment results show the effective extraction of spectral information from CS signals by the proposed framework, and the DCT basis matrix provides the most accurate results while minimizing estimation variances. The execution time is also reduced compared with that of the traditional approach, which completely reconstructs the original data.

Conclusion The proposed method provides accurate spectral analysis without full reconstruction. Since it effectively utilizes the data storage and reduces the processing time, it could be applied to small and portable ultrasound systems using the CS technique.

Keywords Compressed sensing · Ultrasound · Attenuation coefficient · Reference phantom method

Introduction

Quantitative analysis of medical ultrasound signals has been consistently studied for several decades to obtain the pathological conditions of scanned soft tissues in terms of sound speed, scatterer density or size, and backscatter coefficients [1–5]. Among the various ultrasound parameters, the ultrasound attenuation property is basically related to the tissue medical status, and also provides quantitative information for analysis of other ultrasound parameters. However, since the time gain compensation (TGC) method accounts for the attenuation rate of backscattered signals simply according to the depth, it exhibits some drawbacks such as enhancement or shadowing effects in regions comprising different attenuation characteristics [3]. Therefore, numerous researches have been actively attempting to estimate attenuation coefficients accurately, and to examine the physical states of the human organs, including the liver [6], kidney [7], bone [8, 9], and chest [10].

Estimation algorithms of ultrasound attenuation coefficients can be classified according to the methods of the frequency domain and the time domain. For the algorithms in the time domain, Flax et al. showed the potential application of measurement of the zero-crossing density of backscattered ultrasound signals for estimation of attenuation coefficients [11]. Further, Greenleaf and He employed the local maximum of the echo signal envelope to estimate attenuation coefficients [12], while Jang et al. proposed a method for measurement of the entropy differences between two adjacent segments of narrowband echo signals [13]. Video signal analysis (VSA) methods were developed by Knipp et al. to estimate attenuation coefficients directly from B-mode images [14]. Regarding the frequency-domain methods, Yao et al. developed the reference phantom method (RPM) to effectively compensate for the hardware properties of the

✉ Hyungsuk Kim
hskim@kw.ac.kr

[1] Department of Electrical Engineering, Kwangwoon University, Wolgye-dong Nowon-gu, Seoul 139-701, Korea

ultrasound system and the diffraction effects that are due to the beam focus [15]. Fink et al. developed the centroid downshift method by using the short-time Fourier analysis techniques for estimation of the spectral shift, which is related to the attenuation properties [16]. Kim and Varghese suggested a hybrid method that combines the spectral-difference and spectral-shift approaches using spectral cross-correlation and Gaussian filtering [17].

While the estimation performance of medical ultrasound parameters has been important for quantitative ultrasound analysis, the acquisition time and storage of the received ultrasound data have also increasingly received attention recently. The sampling frequency of modern medical ultrasound systems is much higher than the Shannon–Nyquist sampling rate for both the finer spatial and frequency resolutions. Research on three-dimensional representations of two-dimensional (2-D) transducer arrays also requires larger data storage and faster data acquisition with respect to data scanning [18]. In addition, for portable diagnostic ultrasound equipment, reduction of the hardware size and cost regarding data storage and time is one of the important practical issues in terms of implementation of a real-time system [19].

In terms of reduction of data storage and acquisition time, the compressed sensing (CS) technique has emerged as an alternative solution since it can reconstruct the original signal using fewer data samples, which are acquired at sampling rates that are lower than the Shannon–Nyquist sampling theory under the assumption of the sparsity of the original signals. Therefore, the CS technique has been actively applied in the field of medical ultrasound signal processing to improve acquisition times and effectively use data storage space [20–23].

In MRI research fields, the data acquisition time is dynamically reduced by the CS technique [24]. However, because medical ultrasound is a real-time diagnostic system, we focused on reducing hardware size and data storage for portable diagnostic systems by reducing the sampling rate with the CS theory.

In cases where compressed sensing signals are processed for quantitative analysis, however, the reconstruction process that fully recovers the CS data into the original signals in the time domain should be first fulfilled before application of other signal processing techniques.

In the present paper, a spectral analysis framework is proposed for CS ultrasound data; here, the spectral properties are directly extracted without full transformation of time-domain signals into those of the frequency domain. Generally, to estimate spectral information from time-domain signals, the signals need to be transformed from the time domain into the frequency domain using a transformation technique such as fast Fourier transform (FFT). The proposed method, however, directly calculates the frequency information from the CS data while reconstructing it. Derivation of the CS theory furnishes the appropriate basis matrix [25], and provides the spectral information of the CS data in the reconstruction process. To validate the proposed framework, attenuation coefficients are estimated from the CS ultrasound data using the RPM together with the spectral information that is directly extracted using the proposed method. Additionally, the estimation performance of three different basis matrices—discrete Fourier transform (DFT), discrete cosine transform (DCT), and discrete wavelet transform (DWT)—is compared to select the proper basis for the reconstruction process.

The results of simulations and experiments, for which a uniformly attenuating tissue-mimicking (TM) phantom was used, show the proper functionality of the proposed spectral analysis framework with the CS data at a variety of compression rates. Regarding the reconstruction basis matrix, the DCT basis matrix exhibits the best estimation results in terms of accuracy and precision. Since the proposed method does not completely recover the CS data in the estimation of the attenuation coefficients, the execution time is also faster than with full reconstruction.

This paper is organized as follows. The next section briefly summarizes the CS technique and the RPM, as well as presenting the details of the proposed techniques and experimental procedures. Section "Results" considers the TM phantom experiment results in a comparison of the estimation performance of the three basis matrices (DCT, DFT, and DWT) at a variety of compression rates of the CS data. The final section discusses several aspects of the proposed techniques and summarizes the contributions of this paper.

Materials and methods

Compressed sensing technique

According to the Shannon–Nyquist sampling theory, the sampling rate for the conversion of analog signals to discrete-time signals must be at least twice as fast as the original signal maximum frequency to completely recover the discrete-time signals into the original ones [26, 27]. The CS technique, however, has proved that undersampled discrete-time signals, for which the sampling rate is lower than the Shannon–Nyquist sampling rate, could be almost completely recovered if the original signals satisfy the two conditions of sparsity and incoherence [25]. If the number of non-zero values of the original signals is K, the signal can be expressed with K-sparse signal [25].

Regarding the mathematical forms, commencement of the CS technique may be the signal representation according to the following equation:

$$y = \mathbf{A}x, \tag{1}$$

where the vector $y(M \times 1)$ is the measured signal that is compressively sampled from the original signal $x(N \times 1)$ with the measurement matrix $\mathbf{A}(N \times M)$.

Figure 1a is a simplified schematic of the compressed sensing theory. The measurement matrix A compresses the original signal x by 50% to obtain the compressed signal y.

A generally accounts for the matrix with the Bernoulli random distribution or the Gaussian random distribution. If the original signal is K-sparse and M satisfies the condition of $M \geq O(K \log (N/K))$ in **A**, x may be almost completely recovered from the compressed sensing signaly. Although x is not sparse in this domain, a specific transformation could make it a sparse signal in the other domain. Then x in Eq. (1) can be expressed as follows:

$$x = \mathbf{B}^{-1} f, \tag{2}$$

where the matrix $\mathbf{B}(N \times N)$ is a basis (transformation) matrix comprising an inverse matrix, and the vector $f(N \times 1)$ is the coefficient of the specific **B**. To apply the CS theory, the basis matrix should be chosen to satisfy the K-sparse condition for the vector f.

In this case, Eq. (1) can be rewritten with the matrix **T**, as follows:

$$y = \mathbf{A}\mathbf{B}^{-1} f = \mathbf{T} f \quad \text{where } \mathbf{T} = \mathbf{A}\mathbf{B}^{-1}. \tag{3}$$

In Fig. 1b, although x is not sparse in the time domain, the DCT basis matrix could make this original signal a sparse one in the frequency domain.

According to Eq. (3), the vector f is first calculated from the undersampled y to recover x using Eq. (2). In general, the number of solutions of Eq. (3) will be infinite since this problem is underdetermined. If **T** is satisfied with the restricted isometry property (RIP) condition, however, as shown in Eq. (4), it becomes possible to determine the unique solution using optimization techniques such as linear programming.

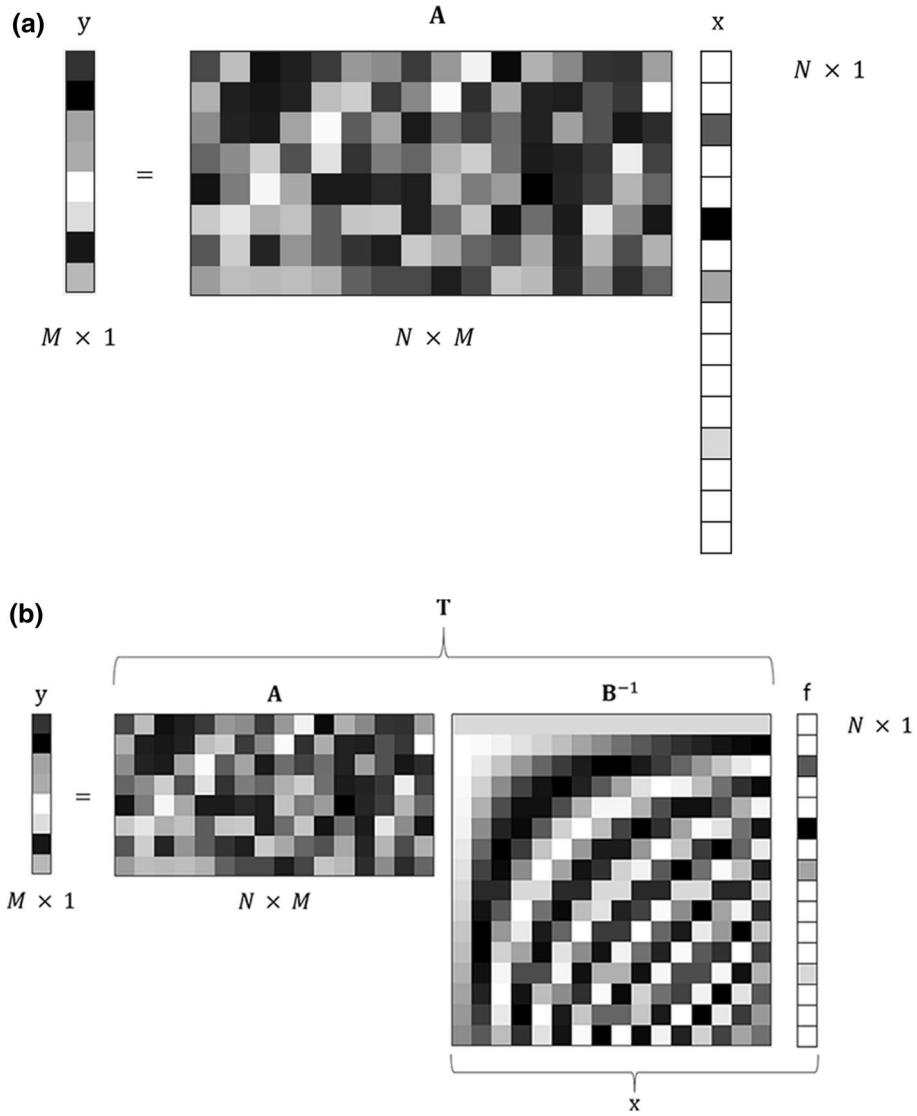

Fig. 1 **a** Compressed sensing theory and **b** compressed sensing theory with DCT basis matrix

$$\left(1-\delta_{2K}\right)||f||_2 \le ||\mathbf{T}f||_2 \le \left(1-\delta_{2K}\right)||f||_2. \quad (4)$$

If $\mathbf{T}$ satisfies the above RIP conditions, the solution can be obtained using l_0-minimization. However, l_0-minimization is not practical since it is the nondeterministic polynomial-time (NP)-hardness problem [28] that must be fully checked for the K-sparse vector. Alternatively, l_1-minimization is the convex optimization problem [29] in the following Eq. (5), enabling the solving of the problem according to the linear problem [30]:

$$\bar{f} = \text{argmin}||f||_1 \quad \text{subject to } \mathbf{T}f = y. \quad (5)$$

Reference Phantom Method (RPM)

The RPM is the estimation algorithm for ultrasound attenuation coefficients. It uses the ratio of the power spectra between the reference phantom, the attenuation properties that are already known, and the sample in the frequency domain [15]. Since the RPM effectively eliminates the system-dependent parameters such as the pulse shape and the diffraction effect, it achieves reliable estimation performance in the uniform-attenuation regions. The brief mathematical equations are subsequently presented.

For quantitative analysis of medical ultrasound signals, the intensity of the reflected signal $I(f,z)$ can be modeled as the product of four characteristic terms in the frequency domain, as follows:

$$I(f,z) = G(f)\cdot D(f,z)\cdot A(f,z)\cdot B(f), \quad (6)$$

where $G(f)$ is the characteristic of the transmitted pulse function, $D(f,z)$ is the diffraction effect, $A(f,z)$ is the attenuation characteristics, and $B(f)$ is the backscatter properties of a certain depth z. The RPM calculates the ratio of the sample intensities to those of the reference signals in the frequency domain to estimate the attenuation and backscatterer coefficients. Since $G(f)$ and $D(f,z)$ are system-dependent properties, the actual tissue characteristics of the scanned region, $A(f,z)$ and $B(f)$, can be obtained using the ratio of the reference signals to the sample signals; at a given echo depth, this ratio measurement can be represented as follows:

$$\begin{aligned}\text{RI}(f,z) &= \frac{I_s(f,z)}{I_r(f,z)} = \frac{G(f)D(f,z)A_s(f,z)B_s(f)}{G(f)D(f,z)A_r(f,z)B_r(f)} \\ &= \frac{B_s(f)}{B_r(f)}\exp\left\{-4\left(\beta_s-\beta_r\right)fz\right\}\end{aligned}. \quad (7)$$

To separate the attenuation and backscatterer terms, the logarithm of Eq. (7) is used, as follows:

$$L(f,z) = \log \text{RI}(f,z) = \log\frac{B_s(f)}{B_r(f)} + 4\left(\beta_r-\beta_s\right)fz. \quad (8)$$

Since the term of $\log\frac{B_s(f)}{B_r(f)}$ is constant, the difference between the attenuation coefficients of the reference and sample signals, denoted by $\beta_r-\beta_s$, can be estimated using linear regression along z, as shown in the following Eq. (9):

$$\beta_\Delta(f) = \beta_r-\beta_s = \frac{1}{4f}\frac{dL(f,z)}{dz} \quad (9)$$

Spectral analysis framework for CS signals

Most of the quantitative analyzes of medical ultrasound are performed in the frequency domain, where extraction (or estimation) of the spectral properties from the reflected time-domain signals should be the first step for further processing. While FFT provides a sound framework to convert time-domain signals into frequency-domain signals, it cannot be directly applied to CS data. That is, while CS signals are advantageous with respect to the acquisition and storage processes in terms of time and space, they should be fully restored into time-domain signals before processing of the spectral analysis in the frequency domain.

In this paper, the proposed spectral analysis framework for CS ultrasound signals involves the direct estimation of spectral properties without restoration of measured signals into full time-domain signals. Since the basis matrix of the CS theory is used for conversion of original signals into spare signals, its coefficients already contain the spectral information of the original signals if the appropriate basis matrix is applied. The proposed method calculates the frequency information from the CS data during the reconstruction process of Eq. (5), so the redundant transformation from the time domain into the frequency domain is not needed. To validate the proposed spectral framework for CS signals, attenuation coefficients are estimated using the RPM with the spectral information, which is directly extracted during the restoration of the CS data.

Figure 2 shows the two procedures for attenuation coefficient estimation with the CS ultrasound signals, where the traditional method and the proposed framework are used. While the dotted line represents the transforming of the time-domain signals into those of the frequency domain by the traditional approach after full reconstruction, the solid line represents the proposed spectral analysis framework for which transformation of the CS signals is not implemented. To compare the estimation performance of the basis matrices, three different basis matrices are applied to the reconstruction process. The CS ultrasound signal is reconstructed using the l_1-norm minimization algorithm for simplicity.

Experiment procedures

To validate the proposed framework, the attenuation coefficients are estimated from the CS ultrasound data using the

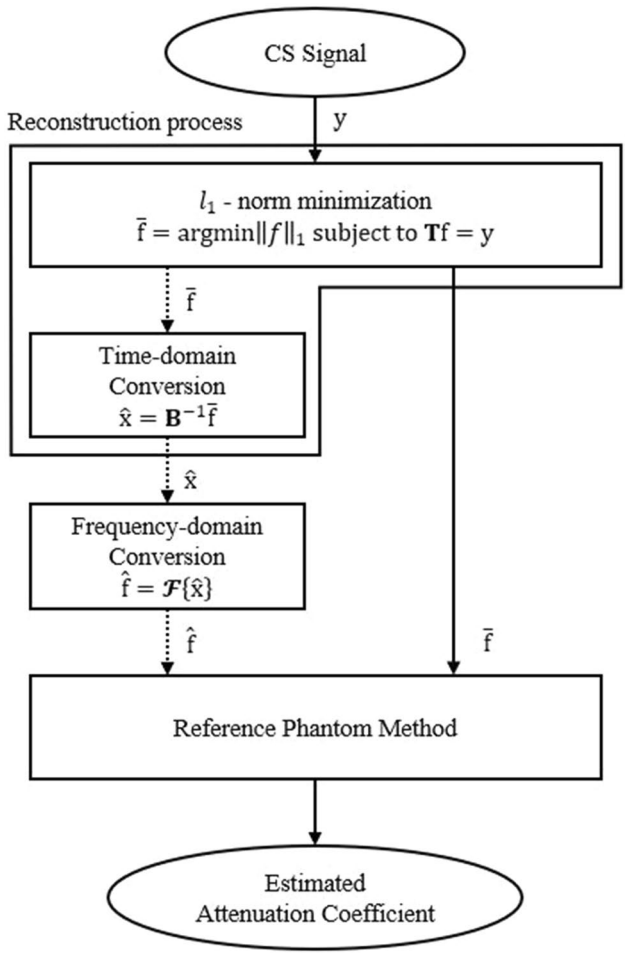

Fig. 2 Traditional approach (dotted line) and the proposed framework (solid line) for spectral analysis with compressed sensing signals

Table 1 Sparsity level of each basis matrix

	256 points (%)	512 points (%)	1024 points (%)
DCT	16	13	14
FT	19	18	15
DWT	22	19	17

RPM together with the spectral information that is directly extracted using the proposed method. Additionally, the estimation performance of three different basis matrices—DFT, DCT, and DWT—is compared to select the proper basis for the reconstruction process. Table 1 shows the sparsity level of original signal x in the frequency domain through each basis matrix. If the number of non-zero values of the original signals is K, the signal is K-sparse signal. Table 1 represents a percentage of non-zero signals for the entire signal through each basis matrix when the length of the signal is 256, 512, and 1024 points. In this table, DCT basis makes the signal more sparse in our case.

Simulated uniform phantoms

Two uniform numerical phantoms were simulated using a C++ program for evaluation of the performance of the proposed method. One was a uniform reference phantom with an attenuation coefficient of 0.7 dB/cm/MHz through the overall depth, and the other was a sample phantom with an attenuation coefficient of 0.5 dB/cm/MHz through the overall depth. The center frequency of the transmit pulse was 5 MHz with a bandwidth of 80%, and the beam focus was set to 4 cm. To estimate the local spectral information, the whole ultrasound radiofrequency signal was divided into small blocks with the dimension of 4×4 mm, and an overlap ratio of 80% is applied to both the axial and lateral directions to obtain finer spatial resolution.

The CS signals were obtained using application of the measurement matrix of the Gaussian random distribution to the individual A-line data of the original signal, as shown in Eq. (1). In this paper, the original signals were compressively sensed with different compression rates from 50–90% to compare the attenuation coefficient estimation performance. The length of original signal x was 512 points in the time domain to the axial direction. The length of compressed sensing signal y was 256 points, 204 points, 153 points, 102 points, and 51 points, respectively.

The three basis matrices, DCT, DFT, and DWT, were applied to the CS signals to extract the spectral information. To determine the unique solution to Eq. (5) during the restoration process, l_1-norm minimization, which is based on the standard interior point method and the convex-optimization method, was employed.

3-Layered TM phantoms

Two TM phantoms were scanned using the Siemens Antares ultrasound system (Siemens Medical Systems, USA) for evaluation of the performance of the proposed method. One was a uniform reference phantom with an attenuation coefficient of 0.5 dB/cm/MHz through the overall depth, and the other was a sample phantom, called a three-layer phantom, consisting of different attenuating regions while the same backscatter properties were maintained. The attenuation coefficients of the sample phantom were 0.5 dB/cm/MHz (0– 4 cm), 0.7 dB/cm/MHz (4–5.5 cm), and 0.5 dB/cm/MHz (5.5–7 cm) through the axial depth. Figure 3 shows the B-mode images of the reference and sample TM phantoms, respectively.

The experiment was conducted in the same way as in the previous simulated numerical phantom experiment.

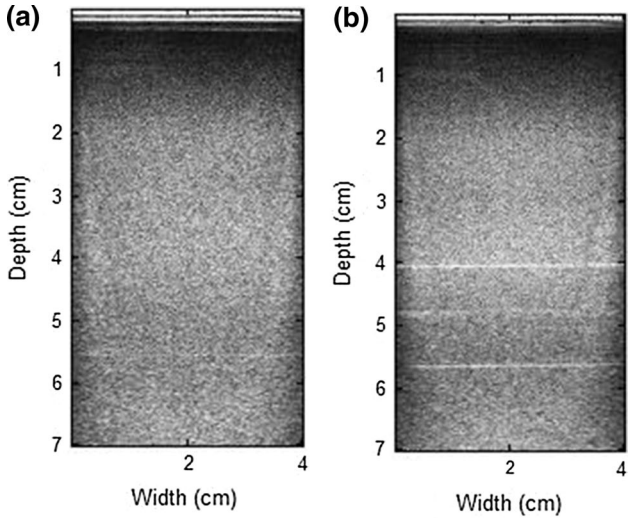

Fig. 3 B-mode images of reference and sample TM phantoms: **a** uniform reference TM phantom with an attenuation coefficient of 0.5 dB/cm/MHz and **b** three-layer sample TM phantom with attenuation coefficients of 0.5 dB/cm/MHz (0–4 cm), 0.7 dB/cm/MHz (4–5.5 cm), and 0.5 dB/cm/MHz (5.5–7 cm)

Results

To verify the proposed spectral analysis framework, attenuation coefficients were estimated from CS ultrasound signals using the RPM with three different basis matrices. Calculation of the fully restored signals provided the best attenuation coefficient estimation results for comparison of the estimation performance of CS data.

Simulated uniform phantoms

Figure 4 shows the estimation results of attenuation coefficients from CS ultrasound data for the three basis matrices using uniform numerical phantoms. For comparison purposes, the theoretical values of the attenuation coefficients of the uniform phantom were plotted in the same graph with dotted lines. The estimated attenuation coefficients of the DCT basis matrix exhibited the best results for the entire depth compared with the other matrices. The estimated values of the DFT and DWT basis matrices were underestimated along the depth.

Figure 5 shows the estimation performance of the DCT basis matrix for the compression rates of 50, 70, and 90%. The 50% compression rate provided reliable estimation results for the entire depth compared with theoretical cases. As the compression rate increased, the estimation accuracy significantly decreased.

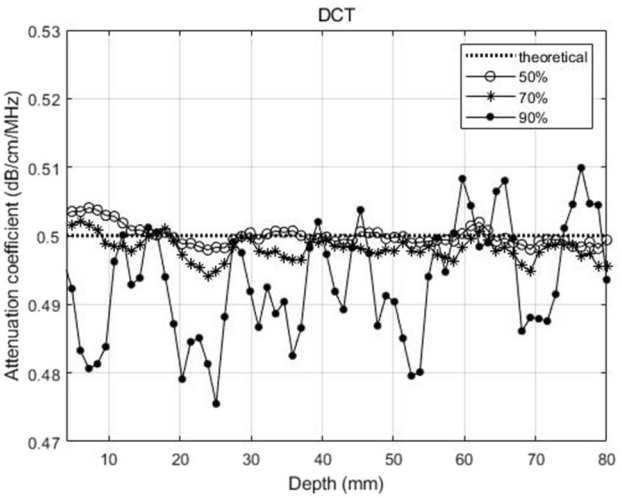

Fig. 4 Estimation results of the numerical phantom attenuation coefficients for different compression rates using the DCT basis matrix

3-layer TM phantoms

Figure 6 shows the estimation results of attenuation coefficients from CS ultrasound data for which the three basis matrices were used. CS ultrasound signals with a compression rate of 50% were utilized, and the estimated attenuation coefficients were averaged laterally at the same depth. For comparison purposes, the theoretical values of the attenuation coefficients of the three-layer TM phantom and the estimated attenuation coefficients with the fully reconstructed signals, labeled "FULL," were also plotted in the same graph. The estimated attenuation coefficients of the DCT basis matrix exhibited the best results for the entire depth compared with the other matrices. The estimated values of

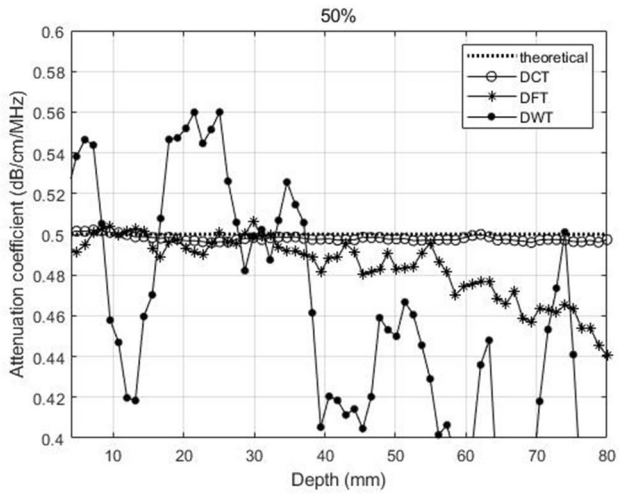

Fig. 5 Estimation results of the numerical phantom attenuation coefficients for three basis matrices with a compression rate of 50%

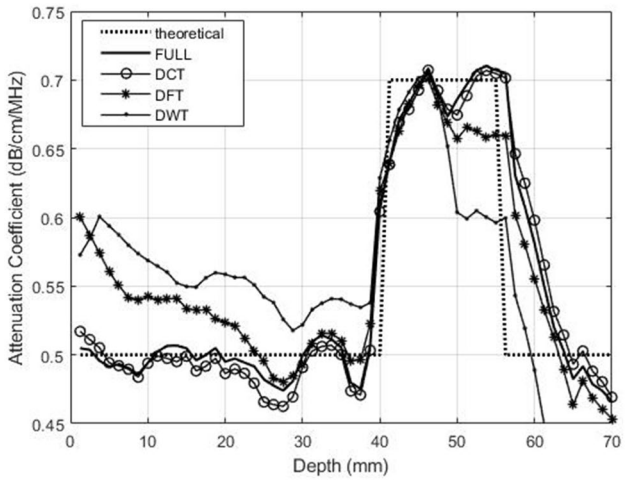

Fig. 6 Estimation results of the 3-layer TM phantom attenuation coefficients for three basis matrices with a compression rate of 50%

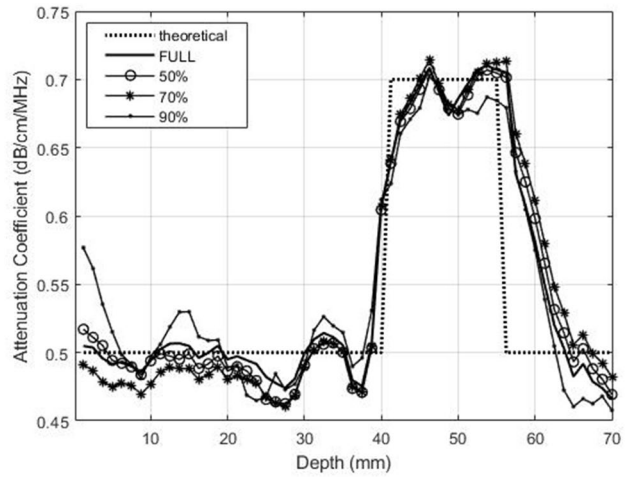

Fig. 7 Estimation results of the 3-layer TM phantom attenuation coefficients for different compression rates using the DCT basis matrix

the DFT and DWT basis matrices were overestimated prior to the beam focus and underestimated after the focus along the depth. When the same number of CS data points was used in the reconstruction process, the DCT basis matrix showed more accurate estimation values since it provided a more effective spectral resolution compared with DFT. For the DWT basis matrix, especially after the beam focus, the estimation accuracy tended to be significantly degraded, because the DWT transform coefficient might have been unsuitable for representation of the measured-signal spectral information.

Figure 7 shows the estimation performance of the DCT basis matrix for the compression rates of 50, 70, and 90%. The 50% compression rate provided reliable estimation results for the entire depth compared with those of FULL. As the compression rate increased, the estimation accuracy significantly decreased.

Table 2 Root mean square error (RMSE) of the estimation results of the 3-layer TM phantom for three basis matrices

	50%	60%	70%	80%	90%
Region A (2.5–4 cm) DCT	0.00278	0.00802	0.00839	0.00949	0.01162
DFT	0.01030	0.01528	0.02257	0.03217	0.03954
DWT	0.04038	0.04432	0.04906	0.05879	0.07237
Region B (4–5.5 cm)					
DCT	0.00801	0.00952	0.01031	0.01219	0.01464
DFT	0.01625	0.02304	0.02774	0.03472	0.04185
DWT	0.04815	0.05181	0.05633	0.05783	0.06981

Table 3 Standard deviations of the estimation results of the 3-layer TM phantom for three basis matrices

	50%	60%	70%	80%	90%
DCT	0.02325	0.02380	0.02603	0.02916	0.07549
DFT	0.02600	0.02687	0.02779	0.03019	0.07916
DWT	0.02548	0.02704	0.02978	0.03617	0.07617

To compare the estimation performance quantitatively, two regions were selected before/after the beam focus for which the attenuation coefficients were different. One of the regions, called "Region A," was between the depths of 2.5 cm and 4 cm, and the other region, "Region B," was between the depths of 4 cm and 5.5 cm, while the attenuation coefficients of each were 0.5 dB/cm/MHz and 0.7 dB/cm/MHz, respectively. The third layer (5.5–7 cm) was far from the transducer and after the beam focus, so it was not included in the quantitative comparison due to its relatively lower signal-to-noise ratio (SNR).

Table 2 shows the root mean square error (RMSE) of the estimated attenuation coefficients for the various compression rates of each region. In Region A, the DCT basis matrix showed the lowest RMSE for all the compression rates. Although the estimation errors also increased as the compression rates increased, it produced relatively small errors of approximately 0.002–0.01. As shown in Fig. 3, for the DFT and DWT basis matrices, the RMSE was larger compared with that for DCT, and a greater estimation error became evident as the compression rates increased. Notably, the same tendency was exhibited for Region B.

Table 3 shows the average standard deviations of the estimation results according to the different compression rates, thereby providing the guideline for the selection of

Table 4 Comparison of the relative computational times with the DCT basis matrix

	50%	60%	70%	80%	90%
Proposed framework	1.37378	1.30402	1.19097	1.12242	1.00000
Traditional approach	2.08742	2.00838	1.85330	1.72084	1.63578

the acceptable compression rate when the CS technique is applied to medical ultrasound spectral analysis. For the overall estimation performance, as shown in Fig. 4, the DCT basis matrix produced the least errors for all the compression rates; however, at the 90% compression rate, the standard deviation rapidly increased. Although the RMSE results were reasonable at this compression rate, the standard deviation was not acceptable with respect to the estimation precision. Because both the precision and the accuracy are important in medical ultrasound quantitative analysis, the appropriate compression rate should account for the tradeoff between the data size and the estimation performance.

Table 4 shows the relative computational times of the traditional approach (full reconstruction for CS data) and the proposed spectral analysis framework with the DCT basis matrix. The computer simulations were performed using the Matlab program (version 9.2) on an Intel i5-2500 (3.3 GHz) system. Note that the computational time was normalized by the shortest one, i.e., the time of the proposed method with the compression rate of 90%. Since the transformation process (e.g., FFT) was omitted, the proposed framework was faster than the traditional approach. As for data storage, the proposed framework was more efficient than the traditional approach since it was not necessary to accommodate the fully restored signal.

Discussion

This paper presents a proposal for a spectral analysis framework for CS ultrasound signals that directly extracts the frequency properties without restoring the measured signals into the full time-domain signals. While most spectral analysis techniques first transform the time-domain signals into frequency-domain signals using the FFT method, the proposed CS signal framework directly uses the spectral information in the recovery process by the proper basis matrix before completely recovering the full signals in the time domain.

Comparative analysis of the respective attenuation coefficient estimations, for which the DCT, DFT, and DWT matrices were used as the basis matrices of the CS technique, showed the superiority of the estimation performance of the DCT basis matrix in terms of accuracy and precision. While a lower compression rate provided more accurate estimation results, acceptable estimation performance was obtained up to the compression rate of 80% in the authors' experiment. The execution time of the proposed framework for ultrasound quantitative analysis was also reduced since it did not completely restore the time-domain signals. The proposed framework can be effectively applied to CS data for small and portable ultrasound systems and applications.

Conclusion

Spectral analysis of medical ultrasound has been actively studied to provide quantitative information on various under-examination ultrasound parameters, and also to suggest a basis for a more precise judgment of pathological states. In particular, the attenuation coefficient of medical ultrasound signals is one of the most important quantitative information that precedes the accurate estimation of other ultrasound indices.

In this paper, a spectral analysis framework was proposed for CS ultrasound data. The spectral properties were directly extracted without full transformation of the time-domain signals into those of the frequency domain.

In conclusion, the proposed spectral analysis framework can be effectively applied to CS data for small and portable ultrasound systems and applications.

Acknowledgements This work was supported by the Korea Institute of Energy Technology Evaluation and Planning (KETEP); the Ministry of Trade, Industry & Energy (MOTIE) of the Republic of Korea (No. 20174010201620); the National Research Foundation of Korea through the Ministry of Education and Ministry of Science (NRF-2017R1D1A1B03034733); and research grant of Kwangwoon University.

Compliance with ethical standards

Conflict of interest We declare that we have no conflicts of interest in connection with this paper.

Ethical statements This article does not contain any studies with human or animal subjects performed by the any of the authors.

References

1. Techavipoo U, Varghese T, Chen Q, et al. Temperature dependence of ultrasonic propagation speed and attenuation in excised canine liver tissue measured using transmitted and reflected pulses. J Acoust Soc Am. 2004;115:2859–65.
2. Wear KA, Stiles TA, Frank GR, et al. Interlaboratory comparison of ultrasonic backscatter coefficient measurements from 2 to 9 MHz. J Ultrasound Med. 2005;24:1235–50.

3. Treece G, Prager R, Gee A. Ultrasound attenuation measurement in the presence of scatterer variation for reduction of shadowing and enhancement. IEEE Trans UFFC. 2005;52:2346–60.
4. Levy Y, Agnon Y, Azhari H. Measurement of speed of sound dispersion in soft tissues using a double frequency continuous wave method. Ultrasound Med Biol. 2006;32:1065–71.
5. Bridal SL, Fournier C, Coron A, et al. Ultrasonic backscatter and attenuation (11–27 MHz) variation with collagen fiber distribution in ex vivo human dermis. Ultrason Imaging. 2006;28:23–40.
6. Fujii Y, Taniguchi N, Itoh K, et al. A new method for attenuation coefficient measurement in the liver: comparison with the spectral shift central frequency method. J Ultrasound Med. 2002;21:783–8.
7. Lee K. Dependences of the attenuation and the backscatter coefficients on the frequency and the porosity in bovine trabecular bone: application of the binary mixture model. J Korean Phys Soc. 2012;60:371–5.
8. Wear KA. Characterization of trabecular bone using the backscattered spectral centroid shift Characterization of trabecular bone using the backscattered spectral centroid shift. IEEE Trans UFFC. 2003;50:402–7.
9. Nagatani Y, Mizuno K, Saeki T, et al. Numerical and experimental study on the wave attenuation in bone—FDTD simulation of ultrasound propagation in cancellous bone. Ultrasonics. 2007;48:607–12.
10. Nam K, Zagzebski JA, Hall TJ. Quantitative assessment of in vivo breast masses using ultrasound attenuation and backscatter. Ultrason Imaging. 2013;35:146–61.
11. Flax SW, Pelc NJ, Glover GH, et al. Spectral characterization and attenuation measurements in ultrasound. Ultrason Imaging. 1983;5:95–116.
12. He P, Greenleaf JF. Application of stochastic-analysis to ultrasonic echoes—estimation of attenuation and tissue heterogeneity from peaks of echo envelope. J Ultrasound Med. 1986;79:526–34.
13. Jang HS, Song TK, Park SB. Ultrasound attenuation estimation in soft tissue using the entropy difference of pulsed echoes between two adjacent envelope segments. Ultrason Imaging. 1988;10:248–64.
14. Knipp BS, Zagzebski JA, Wilson TA, et al. Attenuation and backscatter estimation using video signal analysis applied to B-mode images. Ultrason Imaging. 1997;19:221–33.
15. Yao LX, Zagzebski JA, Madsen EL. Backscatter coefficient measurements using a reference phantom to extract depth-dependent instrumentation factors. Ultrason Imaging. 1990;12:58–70.
16. Fink M, Hottier F, Cardoso JF. Ultrasonic signal processing for in vivo attenuation measurement: short time Fourier analysis. Ultrason Imaging. 1983;5:117–35.
17. Kim H, Varghese T. Hybrid spectral domain method for attenuation slope estimation. Ultrasound Med Biol. 2008;34:1808–19.
18. Huang Q, Zeng Z. A Review on real-time 3D ultrasound imaging technology. Biomed Res Int. 2017. https://doi.org/10.1155/2017/6027029.
19. Nguyen MM, Mung J, Yen JT. Fresnel-based beamforming for low-cost portable ultrasound. IEEE Trans UFFC. 2011;58:112–21.
20. Schiffner MF, Jansen T, Schmitz G. Compressed sensing for fast image acquisition in pulse-echo ultrasound. Biomed Tech. 2012;57:192–5.
21. Liebgott H, Basarab A, Kouame D, et al. Compressive sensing in medical ultrasound. Proc IEEE Ultrason Symp. https://doi.org/10.1109/ULTSYM.2012.0486.
22. Liebgott H, Prost R, Friboulet D. Pre-beamformed RF signal reconstruction in medical ultrasound using compressive sensing. Ultrasonics. 2013;53:525–33.
23. Chernyakova T, Eldar Y. Fourier-domain beamforming: The path to compressed ultrasound imaging. IEEE Trans UFFC. 2014;61:1252–67.
24. Lustig M, Donoho D, Pauly JM. Sparse MRI: The application of compressed sensing for rapid MR imaging. Magn Reson Med. 2007;58:1182–95.
25. Donoho D. Compressed sensing. IEEE Trans Inf Theory. 2006;52:1289–306.
26. Nyquist H. Certain topics in telegraph transmission theory. AIEE Trans. 1928;47:617–44.
27. Shannon C. Communication in the Presence of Noise. Proc IRE. 1949;37:10–211.
28. Knuth DE. Postscript about NP-hard problems. ACM SIGACT News. 1974;6:15–6.
29. Candès EJ, Recht B. Exact matrix completion via convex optimization. Found Comput Math. 2009;9:717–72.
30. Candès EJ, Wakin MB. An introduction to compressive sampling. IEEE Signal Process Mag. 2008;25:21–30.